

# Accurate Internal Camera Calibration using Rotation, with Analysis of Sources of Error

G. P. Stein  
Artificial Intelligence Laboratory  
MIT  
Cambridge, MA, 02139

## Abstract<sup>1</sup>

*This paper describes a simple and accurate method for internal camera calibration based on tracking image features through a sequence of images while the camera undergoes pure rotation. A special calibration object is not required and the method can therefore be used both for laboratory calibration and for self calibration in autonomous robots.*

*Experimental results with real images show that focal length and aspect ratio can be found to within 0.15 percent, and lens distortion error can be reduced to a fraction of a pixel. The location of the principal point and the location of the center of radial distortion can each be found to within a few pixels.*

*We perform a simple analysis to show to what extent the various technical details affect the accuracy of the results. We show that having pure rotation is important if the features are derived from objects close to the camera. In the basic method accurate angle measurement is important. The need to accurately measure the angles can be eliminated by rotating the camera through a complete circle while taking an overlapping sequence of images and using the constraint that the sum of the angles must equal 360 degrees.*

## 1 Introduction:

### 1.1 What is camera calibration ?

Internal camera calibration involves finding the mapping between image coordinates and ray directions in space, which are measured in the camera coordinate system. In practice this often means finding the parameters of the perspective projection model, focal length (or more precisely, principal distance), the principal point, parameters of a lens distortion model and finding the ratio of the spatial sampling of the image plane in the  $X$  and  $Y$  directions (pixel aspect ratio or scale factor). External camera calibration involves finding the position (translation and orientation) of the camera in some world coordinate system.

---

<sup>1</sup>This report describes research done at the Artificial Intelligence Laboratory of the Massachusetts Institute of Technology. Support for the laboratory's artificial intelligence research is provided in part by the Advanced Research Projects Agency of the Department of Defense under Office of Naval Research contract N00014-91-J-4038. Support for Gideon P. Stein is provided by a fellowship from the National Science Foundation.

Camera calibration is important if we wish to derive metric information from the images. Typical applications would be structure from motion and pose estimation which often use the perspective projection model and assume that the internal camera parameters are known [6]. For such work, accurately calibrating the internal camera parameters is critical but the external camera calibration is not important.

### 1.2 Related work

More extensive reviews of calibration methods appear in [9][10][11].

Most techniques for camera calibration use a set of points with known world coordinates (control points). Control points can be from a calibration object [11] or a known outdoor scene [9]. The calibration process can be stated as follows: given a set of control points  $(X_i, Y_i, Z_i)$  and their image  $(x_i, y_i)$  find the external and internal parameters which will best map the control points to their image. A problem arises due to the interaction between the external and the internal parameters. The Manual of Photogrammetry [9] claims that "the strong coupling that exists between interior elements of orientation [principal point and focal length] and exterior elements can be expected to result in unacceptably large variances for these particular projective parameters when recovered on a frame-by-frame basis". The main problem is the error in focal length. For more about this issue see [9][10].

Geometric objects whose images have some characteristic that is invariant to the actual position of the object in space, can be used to calibrate some of the internal camera parameters. Results based on the plumb line method [2], which uses the images of straight lines for calibrating lens distortion, and a method for finding the aspect ratio using spheres [8], are given in section 7 for comparison to the rotation method. More can be found in [10].

Since the traditional methods of camera calibration use known world coordinates they are not suitable for self calibration of mobile robots. To calibrate a camera using only feature coordinates in the image plane one must have more than a single image. Faugeras et al. [4] develop a method where a motion sequence of a camera moving in an unconstrained manner can be used to calculate the internal camera parameters. Simulation results indicate that the method is very sensitive even to small errors in feature location.

Methods that use camera rotation are presented in [1] [3] [5]. Basu [1] tracks the motion of contour lines in the image as the camera pans or tilts through small angles. No lens distortion model is used. The experimental results show that the focal length and scale factor can be found within 3 percent error. No experimental results were given for the principal point. In [3] first the principal point is found and then using the principal point the focal length and scale factor are found, and finally lens distortion parameters. Simulation results show that given features with an accuracy of 0.2 pixels the principal point can be found to within a few pixels and the focal length can be found to within 1 percent. The accuracy of the experimental results are not shown.

The work in [3] is the most closely related to this paper and a comparison is in order. [3] uses three separate stages to recover the camera parameters. In this paper all the parameters are found in one step. The method for finding the focal length presented in [3] (and in [1]) uses small angle approximations to predict the motion of points in the image. On the other hand, for signal to noise reasons, large rotations are required to make accurate measurements. In this paper the full 3D rotation equations are used which are accurate for large and small angles. Finding the radial distortion in [3] requires being able to rotate the camera accurately around the XY axes of the camera. This is a rather complex mechanical setup. In the method presented here, one is only required to be able to rotate about the center of projection.

Recent work by Hartley [5] has shown that given a perfect perspective projection model it is possible in theory to recover both the camera parameters and the angle of rotation. This has been shown to work nicely in simulation but no accuracy results have been shown with real images. The problem is a strong coupling between the focal length and the angle of rotation. An increase in the focal length estimate can be nearly completely compensated for by decreasing the angle estimate. In practice we could not achieve better than 4 percent accuracy in focal length estimates using the iterative method presented in [5].

### 1.3 Brief overview of the rotation method

The basic idea of the rotation method is very simple. Given any pair of images produced by a camera which has undergone pure rotation, if the internal camera parameters and the angle and axis of rotation are known, one can compute where the feature points from one image will appear in the second image of the pair. If there is an error in the internal camera parameters, the features in the second image will not coincide with the feature locations computed from the first image. We take a set of images where the camera has rotated around a fixed axis. We can then find camera parameters that best predict the motion of the feature points in the set of images using nonlinear search. The constraints imposed on the motion result in a calibration method which is very robust to data noise and does not require a good initial guess of camera parameters. For example, nominal values of the camera parameters can be used as the initial starting point for the optimization procedure.

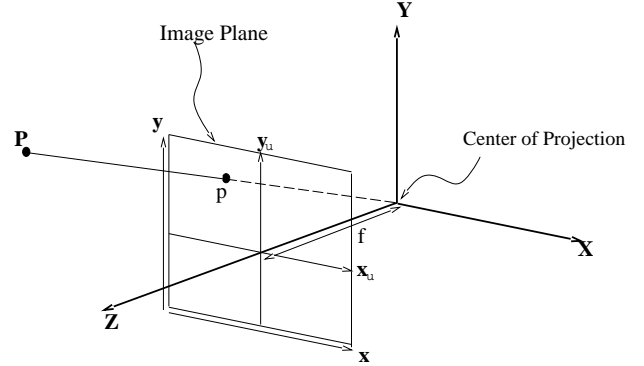


Figure 1: The camera coordinate system  $(X, Y, Z)$ , the undistorted image coordinates  $(x_u, y_u)$  and the frame buffer coordinates  $(x, y)$

Camera lens distortion is taken into account by first correcting the feature coordinates in both images for lens distortion and only then computing the rotated feature points and evaluating the cost function. The lens distortion parameters can be added to the list of parameters to be determined in the non-linear search.

## 2 Mathematical background

### 2.1 The camera model

We use a camera centered Cartesian coordinate system. The image plane is parallel to the  $(X, Y)$  plane and at a distance  $f$  from the origin and the  $Z$  axis coincides with the optical axis (see figure 1). Using perspective projection a point  $\vec{P} = (X, Y, Z)$  in the camera centered coordinate system projects to a point  $p_u = (x_u, y_u)$  on the image plane:

$$\begin{aligned} x_u &= fX/Z \\ y_u &= fY/Z \end{aligned} \quad (1)$$

The  $Z$  axis projects to the point  $(0,0)$  in the image plane which is called the principal point (PP).

The standard model for lens distortion [9] is a mapping from the distorted image coordinates,  $(x_d, y_d)$ , that are observable, to the undistorted image plane coordinates,  $(x_u, y_u)$ :

$$\begin{aligned} x_u &= x_d + x'_d(K_1 r_d'^2 + K_2 r_d'^4 + \dots) \\ y_u &= y_d + y'_d(K_1 r_d'^2 + K_2 r_d'^4 + \dots) \end{aligned} \quad (2)$$

where:

$$r_d'^2 = x_d'^2 + y_d'^2 = (x_d^2 - c_{xr})^2 + (y_d^2 - c_{yr})^2 \quad (3)$$

It has been shown in [10] that allowing the center of radial distortion,  $(c_{xr}, c_{yr})$  to be different from the principal point is equivalent to adding a term for decentering distortion as given in [9]. Finally,  $\vec{P}$  is converted to frame buffer coordinates:

$$\begin{aligned} x &= \frac{1}{S}x_d + c_x \\ y &= y_d + c_y \end{aligned} \quad (4)$$

where  $(c_x, c_y)$  is the principal point in frame buffer coordinates and  $S$  is the aspect ratio or scale factor of the image. One can compute  $S$  using the equation:

$$S = \frac{d_x f_s}{d_y f_p} \quad (5)$$

where  $d_y$  and  $d_x$  are the pixel spacing in the CCD array,  $f_p$  is the camera pixel clock frequency and  $f_s$  is the frame grabber sampling frequency. If any of these values are unknown or variable then  $S$  must be found by calibration. We expect digital cameras to become widely used and the scale factor will be known exactly.

## 2.2 Pure rotation

Given  $\vec{W} = (w_x, w_y, w_z)$ , the axis of rotation and  $(\theta)$ , the angle of rotation one can compute the rotation matrix  $\mathbf{R}(\vec{W}, \theta)$ . If a world point  $\vec{P}$  projects to  $p = (x, y)$  in the image then after rotation  $\vec{P}$  will project to point  $p' = (x', y')$  in the new image.  $x'$  and  $y'$  are given by:

$$\begin{aligned} x' &= f \frac{(r_{11}x + r_{12}y + r_{13}f)}{(r_{31}x + r_{32}y + r_{33}f)} \\ y' &= f \frac{(r_{21}x + r_{22}y + r_{23}f)}{(r_{31}x + r_{32}y + r_{33}f)} \end{aligned} \quad (6)$$

Where  $r_{ij}$  is  $j^{th}$  element along the  $i^{th}$  row of the matrix  $\mathbf{R}$ . The position of the point in the image after rotation depends only on the camera parameters, the rotation  $\mathbf{R}$  and the location of the point in the image before rotation.

## 2.3 Rotation with translation

If the axis of rotation does not pass exactly through the center of projection then there will be some translation  $\vec{T} = (t_x, t_y, t_z)$  in addition to the rotation around the center of projection. In that case the location of an image point after rotation and translation will be:

$$\begin{aligned} x' &= f \frac{(r_{11}x + r_{12}y + r_{13}f + ft_x/Z)}{(r_{31}x + r_{32}y + r_{33}f + ft_z/Z)} \\ y' &= f \frac{(r_{21}x + r_{22}y + r_{23}f + ft_y/Z)}{(r_{31}x + r_{32}y + r_{33}f + ft_z/Z)} \end{aligned} \quad (7)$$

The location of the point is no longer independent of the depth and depends also on the translation vector.

## 3 The rotation method step by step

We take  $M$  pairs of images with the camera rotated at various angles and with the axis of rotation is held constant. The relative angles of rotation are measured precisely. Corresponding features in each of the pairs are found and their coordinates extracted. The number of features found in image pair  $j$  will be denoted  $N_j$ .

The feature coordinates in the distorted image plane can be found using (4):

$$\begin{aligned} x_{d_{ij}} &= S(x_{ij} - c_x) \\ y_{d_{ij}} &= (y_{ij} - c_y) \end{aligned} \quad (8)$$

where  $(x_{ij}, y_{ij})$  are the coordinates of feature  $i$  in image pair  $j$ . We can use (2) to compute the feature coordinates in the undistorted image plane:

$$\begin{aligned} x_{u_{ij}} &= x_{d_{ij}} + \delta x_{d_{ij}} \\ y_{u_{ij}} &= y_{d_{ij}} + \delta y_{d_{ij}} \end{aligned} \quad (9)$$

We can now define a cost function:

$$E = \sum_{j=1}^M \sum_{i=1}^{N_j} ((x'_{u_{ij}} - x_{u_{ij}})^2 + (y'_{u_{ij}} - y_{u_{ij}})^2) \quad (10)$$

where  $(x'_{u_{ij}}, y'_{u_{ij}})$  are the coordinates of  $(x_{u_{ij}}, y_{u_{ij}})$  rotated using (6).

The task is now to find camera parameters  $(f, c_x, c_y, S, K_1, K_2, c_{xr}, c_{yr})$  and the axis of rotation  $\vec{W} = (w_x, w_y, w_z)$  that minimize  $E$  in (10). The parameters are found by nonlinear search. This is not the whole story. To obtain accurate values for the aspect ratio  $S$  it is necessary to use two sets of image pairs each using a different axis of rotation. Ideally both axes should be in the image plane and orthogonal but anything close will do. The vertical ( $Y$ ) axis and the horizontal ( $X$ ) axis are a natural choice. The exact axis of rotation can be found through the minimization of  $E$  in (10). With digital cameras, the aspect ratio is known and then only one set of images is required.

## 4 Experimental details

### 4.1 Hardware

Three B/W CCD cameras were used for the experiments. A Sanyo VDC3860 High Resolution Camera with 8.5 mm and 12.5 mm Comiscar lenses. A Chinon CX-101 Low Resolution camera. This camera has a fixed focus 3 mm lens, a  $\frac{1}{3}$  inch CCD and has an angle of view of  $110^\circ$  along the diagonal. A Pulnix WV-CD 50 high resolution camera with a 16 mm lens. The images were acquired using a Datacube frame-grabber into  $512 \times 485$  frame buffers and processed on a Sparc workstation.

For the rotation experiments the cameras were mounted on an XY stage (DAEDAL model 3972M) which was mounted on a precision rotary stage with a vernier scale that can measure angles to an accuracy of  $\pm 1'$ . ( $1' = \frac{1}{60}^\circ$ ). In practice we found that the repeatability of angular measurements was between  $\pm 1.22'$  [10].

### 4.2 How to obtain pure rotation ?

To obtain pure rotation the camera is mounted on an XY stage that has a fine adjustment. This in turn, is mounted on the rotation stage. The camera can now be positioned so that the axis of rotation passes through the center of projection.

The test whether there is little or no translation is quite simple and was performed experimentally as shown in figure 2. When we rotated the camera, the closer line would move either 'faster' or 'slower' than the other lines. By adjusting the camera position we could make it so that no relative motion could be

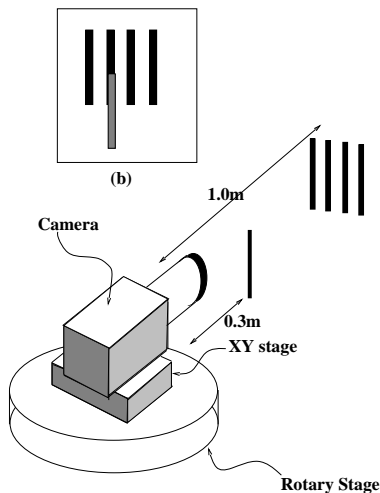


Figure 2: Diagram of the setup used for testing for pure rotation. The camera is mounted on an XY stage that is mounted on a rotary stage. A set of black bars is positioned 1.0m from the camera. A single black bar is positioned about 0.3m from the camera. Its horizontal position is adjusted so that the close bar is aligned with one of the distant bars. The image is viewed on the TV monitor (b).

detected. We found we could position the center of projection less than 0.5 mm from the axis of rotation. For more details see [10].

### 4.3 Features and feature detector

The rotation method does not require any special calibration object but it does require that features can be detected reliably in the image. In order to simplify the feature extraction process we used the corners in a black and white checkerboard pattern printed on  $8 \times 11$  inch paper. The details of the features and feature detector are not critical and are presented fully in [10].

### 4.4 Nonlinear optimization

The camera parameters were found using a nonlinear optimization program based on the subroutine LMDIF from the software package MINPACK-1 [7]. This subroutine uses a modified Levenberg-Marquart algorithm. The program typically takes about 6 iterations to get the first 5 digits and 12 iterations to terminate. For  $M = 10$  and  $N = 20$  this took 11 seconds on a SPARCstation ELC. No attempt was made to optimize the code.

## 5 Rotating a complete circle.

One can avoid the need to measure the rotation angles by using a sequence of images taken as the camera rotates through 360 degrees. Within a large range around the correct angle and focal length, the focal length estimate is a monotonically decreasing function of the angle measurement. This means that given an estimate of the angle, one can obtain an estimate of the focal length and vice versa, given a guess at the focal length, one can obtain an estimate of the angles.

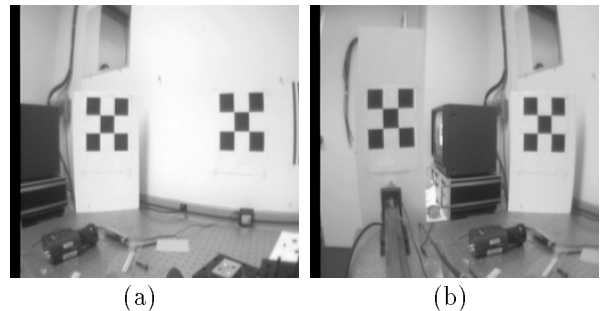


Figure 3: Typical image pair for the full circle rotation method. Image (a) was taken at  $195^\circ$  and image (b) at  $155^\circ$ . Only The checker board pattern in the left of image (a) appears in image (b) on the right hand side.

Let us assume that one has a sequence of  $M$  images taken as the camera rotates through a whole circle and the  $j^{\text{th}}$  image has some area of overlap with the  $j+1^{\text{st}}$  image and that there are some detectable features in each of those areas of overlap. Let us then take the first image in the sequence to be also the last. Each of the  $j^{\text{th}}$  and  $j+1^{\text{st}}$  images can be used as an image pair. For a given guess at the focal length we can obtain an estimate for the angles between the two images in each of the image pairs. We then sum up these angles. If the focal length was guessed correctly then the sum should be 360 degrees. Since each of the angles, and hence the sum of the angles, is a monotonic (decreasing) function of our guess of  $f$ , it is easy to find the correct  $f$  iteratively using numerical methods such as bisection or Brent's method. The other camera parameters do not stay constant as we vary our guess of  $f$  but experimental results show that they vary smoothly. We pick the parameters that correspond to the focal length which gives the correct sum of angles.

A sequence of overlapping images was taken as the camera was rotated to the left in a full circle. Figure 3 shows a typical image pair.

Although the camera used had a wide angle lens and a rotation of 60 degrees would still enable overlap between the images, the camera was not always rotated as much as it could be. If we had done so it would be hard to distinguish between the effects of focal length and radial distortion. So we initially made a few relatively small rotations (5-20 degrees) and we then used large rotations to complete the circle. The images were taken at the following angles: 225, 215, 210, 195, 155, 110, 50, 350, 295, 245, 225, - the same image was used as first and last.

## 6 Analysis of error sources

In this section we will discuss the possible sources of error. This is not a formal error analysis but will give a good idea of how each source of error might affect the results.

### 6.1 Errors in feature detection

If we have an error of 1 pixel in the location of a feature point and the rotation caused a motion of 100 pixels we would expect an error of 1 percent in focal length estimates. But since we use a large number of points, at least 20 per image pair and since the typical errors have zero mean, the final error is much smaller.

### 6.2 Errors caused by not having pure rotation

Let us consider the simple case where the rotation is around the (vertical)  $Y$  axis and that the center of projection is at a distance  $D$  directly behind the axis of rotation. We assume that the  $Z$  axis intersects the axis of rotation. In this case the equation for  $x'$  from (7) becomes:

$$x' = f \frac{(\cos(\theta) * x + \sin(\theta) * f + ft_x/Z)}{(\cos(\theta) * f - \sin(\theta) * x + ft_z/Z)} \quad (11)$$

Where  $t_x = D * \sin(\theta)$  and  $t_z = D * (1 - \cos(\theta))$ . Using the small angle approximation we get  $t_x \simeq D * \theta$  and  $t_z \simeq 0$  and:

$$x' \simeq f \frac{(x + \theta * f + f * D * \theta / Z)}{(f - \theta * x)} \quad (12)$$

Since  $f \gg \theta * x$  we can approximate the above equation to:

$$x' \simeq f \frac{(x + \theta * f + f * D * \theta / Z)}{f} \quad (13)$$

Extracting  $f$  we have:

$$f \simeq \frac{x' - x}{\theta(1 + \frac{D}{Z})} \quad (14)$$

From the above equation we see that for a non zero value of  $D$  we will get an error in the estimate of  $f$ . In fact the error will be  $\frac{D}{Z}$  of the true value. This is a systematic error which cannot be reduced by using many feature points or image pairs. In our case we could ensure that  $D < 0.5mm$  and since  $Z \simeq 1.0m$  the error produced was less than 0.05 percent.

### 6.3 Errors in angle measurement

If we used a single image pair, an error of 1 percent in measurement of the angle would cause an error of 1 percent in the focal length estimate. Since the angle measurements errors are unbiased, taking many measurements can help reduce the error but the standard deviation drops as the square root of the number of image pairs. In our case the angle measurement was estimated to be around  $\frac{1}{50}$  of a degree and with rotation angles of around 20 degrees for the 16 mm lens this would cause an error of 0.1 percent for a single image pair.

In the case of longer focal lengths the possible angle of rotation is smaller and the proportional error in angle measurement is therefore larger. If we use the method of rotating a full circle there is no angle measurement error. Even if we cannot rotate a full circle, due to some mechanical constraint, we could use an image sequence where the total angle is large which is easier to measure with accuracy.

Table 2: Calibration results - using geometric shapes

$f_{[mm]}$	cxr	cyr	k1	k2	sf
Sanyo					
8.5	244.9	245.2	6.07e-07	-1.73e-12	1.2586
Chinon					
3	257.2	229.8	1.80e-6	6.44e-12	1.247

### 6.4 Errors due to radial distortion

In the case of wide angle lenses there can be lens distortion of tens of pixels at the edges. Even in the case of the 16mm lens where the lens distortion was not visible the distortion at the edges of the image was around 3 pixels in an image of  $512 \times 512$  pixels. Since this is a biased error it cannot be overcome by increasing the number of measurements and could, in this case, cause an error of 1 percent in the focal length estimate.

One could try to use points that are located only near the center of the image as in [3]. The effects of radial distortion will be much smaller but that will also limit one to small angle rotations and loss in angle measurement accuracy. As we will only be using the center part of the image the accuracy of the feature detector will also be reduced.

### 6.5 Use of small angle approximations

Both [3] and [1] use small angle approximations to reach closed form solutions for the camera parameters. These approximations,  $\sin(\theta) \simeq \theta$  and  $\cos(\theta) \simeq 1$ , are only good for very small angles. For angles above 10 degrees the error in the cosine approximation is over 1.5 percent and the error in the sine approximation is over 0.5 percent.

## 7 Results

Four experiments were performed with the Sanyo camera and the 8.5mm lens. In each, two sets of images were used, one with horizontal rotation and one with vertical rotation. Each set was made up of nine images taken at various angles. From each set we selected five pairs of images. We used these sets of images to calibrate the camera using the measured angles. We then performed a fifth, similar, experiment with a 12.5mm lens. Between each set of images the camera position was adjusted so that the axis of rotation passed through the center of projection.

With the Chinon camera we performed two experiments using measured angles. We then performed a third experiment (#8 in table 1) where the camera was rotated a full circle and we took an overlapping set of images. This set was used for the full circle rotation method described in section 5. For this third experiment we used only a single set with horizontal rotation. Since this meant that the aspect ratio could not be recovered reliably, we used the average aspect ratio obtained from the first two experiments. The results of the rotation experiments are shown in table 1. For comparison, the results obtained using geometric shapes are summarized in table 2.

We have no ground truth values for the various camera parameters but we can check to see if the

Table 1: Calibration results - using pure rotation

Sanyo Camera										
#	$f_{[mm]}$	$f_{[pixels]}$	cx	cy	cxr	cyr	k1	k2	sf	RMS error
1	8.5	632.4	251.2	243.4	254.1	234.9	5.23e-07	-9.08e-13	1.2583	0.278858
2	8.5	632.4	248.4	245.9	252.6	238.3	5.57e-07	-1.03e-12	1.2576	0.354125
3	8.5	631.8	254.1	240.3	254.8	243.4	5.19e-07	-7.92e-13	1.2567	0.248890
4	8.5	631.3	243.5	248.4	250.1	234.0	5.59e-07	-1.39e-12	1.2552	0.197770
	<i>Mean*</i>	631.95	249.3	244.5	252.9	239.2	5.3958e-07	-1.0303e-12	1.2569	
	$\sigma/\text{mean}$	0.0008	0.0180	0.0142	0.0083	0.0148	0.0403	-0.2511	0.0011	
5	12.5	928.4	244.3	249.9	242.4	233.7	2.239e-07	5.188e-13	1.25741	0.120
Chinon Camera										
#	$f$	cx	cy	cxr	cyr	k1	k2	sf	RMS error	
6	433.5	254.0	225.5	254.2	223.2	1.91e-06	5.41e-12	1.24664	0.43	
7	433.2	249.3	225.3	248.9	221.5	1.88e-06	5.43e-12	1.24721	0.40	
8	431.9	256.3	225.3	254.7	225.7	1.923e-06	3.836e-12	(1.247)	0.922	

\* Mean of experiments 1 though 4.

results are repeatable. For the Sanyo 8.5 mm the standard deviation of the focal length is 0.5 pixels or 0.08%. The standard deviation in aspect ratio,  $S$  is 0.11%. When a 12.5mm lens is used the aspect ratio is the same, as one would hope. The mean for the rotation experiments is 1.2569 which agrees well with the 1.2586 obtained using the spheres. The standard deviation in focal length of the Chinon camera between experiments 6,7 and 8 is 0.85 pixels or about 0.17% of the focal length. The difference between the aspect ratio obtained in experiment 6 and 7 is 0.05% and the mean is 1.2469 which is the same as obtained using spheres.

The variance in the values obtained for the radial distortion parameters  $K_1$  and  $K_2$  using the rotation method is large but the increase of the value of  $K_1$  is compensated for by the decrease in the value of  $K_2$ . Figure 4(a) shows the correction for radial distortion,  $(\delta_x)$ , for the 8.5mm lens as a function of the radial distance from the principal point using the radial distortion parameter values obtained with the plumb line method and with the rotation method. Since we don't know the correct answer, the  $\delta_x$  computed using the parameters obtained from the first rotation experiment is used as ground truth and subtracted from the results obtained using the plumb line method and the other rotation experiments. The results are plotted in Figure 4b. Figure 4c and Figure 4d show similar results for the Chinon camera.

One can see in Figure 4 that the radial distortion coefficients  $K_1$  and  $K_2$  obtained from the rotation and plumb line experiments give the same correction for radial distortion with the difference being less than 0.5 pixels for  $r < 200$ . Using only one term for radial distortion, with the coefficient  $K_1$  obtained by the plumb line method, the correction differs by over 2 pixels for the Chinon camera. Thus it is significantly different and shows that two coefficients must be used. The graphs diverge for  $r > 200$  because the rotation method, as implemented, uses features located along the axes and therefore there is only data for  $r$  less than about 200. This can be corrected by using features near the corners of the images as well.

Table 3: Calibration results - not using pure rotation.  $D$  is the distance of the axis of rotation from the center of projection. The feature patterns were located at a depths from 50cm to 75cm. Note that the RMS error, not just the error in estimated focal length increases with  $D$ .

D	$f_{[pixels]}$	cx	k1	RMS error
0	1260.2	283.958	1.18914e-07	1.551235
3mm	1255.32	272.597	1.04814e-07	1.659607
1cm	1243.36	255.994	1.0223e-07	3.470970
4cm	1178.37	242.397	1.4864e-07	8.937260

With the Pulnix camera we performed an experiment to test the effect of moving the center of projection away from the rotation axis. We used rotation around the Y axis only and used the scale factor which we had found in another experiment not described in this report. We first positioned the center of projection on the axis of rotation and took a set of images. We then moved the center of projection  $D = 3\text{mm}$  away and took a second set of images. We repeated this for  $D = 1\text{cm}$  and  $D \simeq 4\text{cm}$ . For each set of images we found the best camera parameters. We were mainly concerned here with  $f$ . The objects used for feature points were located between 0.5m and 0.75m from the camera.

The results are shown in table 3. When we increase the distance  $D$  the error in focal length  $f$  increases. It is nearly a linear function. We also note that the RMS error increases as  $D$  increases. This is because the depth disparities in the feature objects cause parallax which cannot be modeled by pure rotation. If all the feature points had come from a planar object parallel to the image plane we could have modeled the motion of the points as pure rotation and we would have no indication that something was wrong. The RMS error would be small but the focal length we got would be in error.

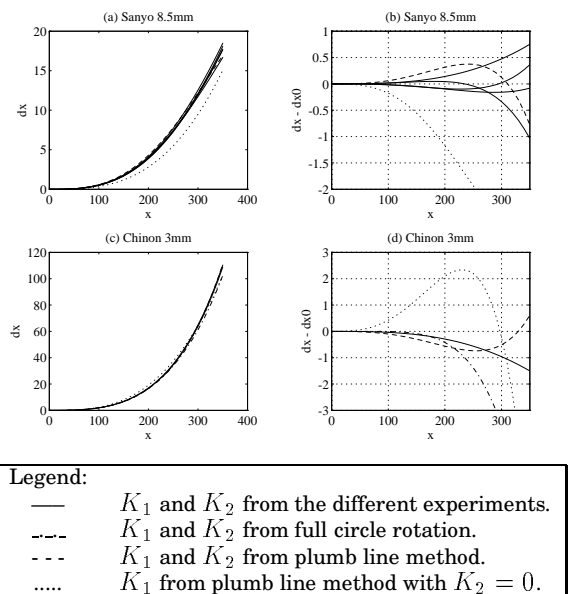


Figure 4: (a) The correction for radial distortion  $\delta_x$  plotted against the distance from the principal point for the Sanyo 8.5mm lens. (b)  $\delta_x$  derived using the average rotation experiment parameters subtracted from the rest of the results in (a). (c) The correction for radial distortion  $\delta_x$  plotted against the distance from the principal point for the Chinon 3mm lens. (d)  $\delta_x$  from the first rotation experiment subtracted from the rest of the results in (c).

## 8 Discussion

The rotation method effectively calibrates the internal parameters of the camera. Using the calibrated camera one can calculate the direction of a ray to a point in space given the coordinates in the image. This direction is given in the camera coordinate system. The calibration method was designed specifically to provide internal camera calibration rather than both internal and external calibration parameters for two reasons. Firstly, in many cases we are interested only in the internal camera parameters and secondly, we avoid the problems involved in decoupling the internal and external parameters.

The rotation method is simple to use because it does not require known world coordinates of control points nor does it require very high precision feature extraction. It is suitable for autonomous robots working in unstructured environments or as a quick and accurate method for calibrating a camera in the laboratory. The most important improvements to the method would be to use a feature detector which can operate in a natural environment and to automatically track the features.

We have shown that with care one can use this method to calibrate the internal parameters to high accuracy. The main issue is pure rotation. More precisely, one must ensure that the deviation from pure rotation is small compared to the distance to the objects. In outdoor scenes, where the objects are far away, this is no problem but indoors one might get errors if one is not careful.

## References

- [1] **Basu, A.**, "Active Calibration: Alternative Strategy and Analysis" In *Proceedings of IEEE Conference on Computer Vision and Pattern recognition*, 495-500, New York, NY, June (1993)
- [2] **Brown, D.C.**, "Close -range Camera Calibration" *Photogrammetric Engineering* **37** 855-866 (1971)
- [3] **Du, F. and Brady, M.**, "Self Calibration of the Intrinsic Parameters of Cameras for Active Vision Systems" In *Proceedings of IEEE Conference on Computer Vision and Pattern recognition*, 477-482, New York, NY, June (1993)
- [4] **Faugeras, O.D., et al.**, "Camera Self-Calibration : Theory and Experiments" In *Proceedings of ECCV*, 321-334, Santa Margherita Ligure, Italy, May (1992)
- [5] **Hartley, R.L.**, "Self-Calibration from Multiple Views with a Rotating Camera" in *Proceedings of the European Conference on Computer Vision* (1994)
- [6] **Longuet-Higgins, H.C.**, "A computer algorithm for reconstructing a scene from two projections" *Nature* **293**,133-135 (1981)
- [7] **More, J.J., et al.**, "User Guide for Minpack-1" Argonne National Laboratory, Argonne, Illinois (1980)
- [8] **Penna, M.A.** "Camera Calibration: A quick and Easy Way to Determine the Scale Factor" *IEEE Trans. Pattern Anal. Machine Intell.* **13**,1240-1245 (1991)
- [9] **Slama, C.C. ed**, *Manual of Photogrammetry*, 4th edition, American Society of Photogrammetry (1980).
- [10] **Stein, G.P.**, "Internal Camera Calibration using Rotation and Geometric Shapes" AITR-1426, Master's Thesis, Massachusetts Institute of Technology, Artificial Intelligence Laboratory (1993).
- [11] **Weng, J et al.** "Camera Calibration with Distortion Models and Accuracy Evaluation" *IEEE Trans. Pattern Anal. Machine Intell.* **14**,965-980 (1992)